COMPUTATION OF MARKET RISK MEASURES WITH STOCHASTIC LIQUIDITY HORIZON

GEMMA COLLDEFORNS-PAPIOL AND LUIS ORTIZ-GRACIA

ABSTRACT. The Basel Committee of Banking Supervision has recently set out the revised standards for minimum capital requirements for market risk. The Committee has focused, among other things, on the two key areas of moving from Value-at-Risk (VaR) to Expected Shortfall (ES) and considering a comprehensive incorporation of the risk of market illiquidity by extending the risk measurement horizon. The estimation of the ES for several trading desks and taking into account different liquidity horizons is computationally very involved. We present a novel numerical method to compute the VaR and ES of a given portfolio within the stochastic holding period framework. Two approaches are considered, the delta-gamma approximation, for modelling the change in value of the portfolio as a quadratic approximation of the change in value of the risk factors, and some of the state-of-the-art stochastic processes for driving the dynamics of the log-value change of the portfolio like the Merton jump-diffusion model and the Kou model. Central to this procedure is the application of the SWIFT method developed for option pricing, that appears to be a very efficient and robust Fourier inversion method for risk management purposes.

Key words. Market Risk, Liquidity Risk, Stochastic Liquidity Horizon, Value-at-Risk, Expected Shortfall, Fourier Transform Inversion, Shannon Wavelets.

AMS subject classifications. 91G60, 62P05, 60E10, 65T60

JEL codes. G13, G32, C63

1. INTRODUCTION

The Basel Committee of Banking Supervision states in the consultative documents [3, 4] that *"the financial crisis exposed material weaknesses in the overall design of the framework for capitalising trading activities. The level of capital required against trading book exposures proved insufficient to absorb losses"*. Within the mentioned documents, the Basel Committee initiated a fundamental review of the trading book regime, beginning with an assessment of those things that went wrong. The revised standards for minimum capital requirements for market risk were recently established in [5].

The Committee has focused, among other things, on the two key areas of moving from VaR to ES and considering a comprehensive incorporation of the risk of market illiquidity. In regard to the first issue, a number of weaknesses have been identified with using VaR for determining regulatory capital requirements, including its inability to capture the risk in the tail. For this reason, the Committee has considered alternative risk metrics like, in particular, the ES, which measures the riskiness of a position by considering both the size and the likelihood of losses above a certain confidence level. The second issue relies on the importance of incorporating the risk of market illiquidity as a key consideration in banks' regulatory capital requirements for trading portfolios. The assumption that trading book risk positions where liquid, i.e., that banks could exit or hedge these positions over a ten-day horizon proved to be false during the recent crisis. As liquidity conditions deteriorated during the crisis, banks were forced to hold risk positions for much longer than originally expected and incurred in large losses due to fluctuations in liquidity premia and associated changes in market prices.

In its deliberations on revising the prudential regime for trading activities, the Committee has drawn on lessons both from the academic literature (see [2]) and banks' current and emerging risk management practices. One of the important messages from the academic literature on risk measurement in the trading book is that there are limitations of VaR models that rely on the use of continuous stochastic processes with only deterministic volatility assumptions. Introducing either stochastic volatility assumptions or stochastic jump process into modelling of risk factors will help to overcome these shortcomings. Another message of paramount importance is that the time it takes to liquidate a risk position varies, depending on its transactions costs, the size of the risk position in the market, the trade execution strategy and market conditions. Some studies suggest that, for some portfolios, this aspect of liquidity risk could also be addressed by extending the VaR risk measurement horizon. These findings are in accordance with those derived from a survey of industry practices in risk management for the trading book carried out by the Committee. As for the length of the holding period, that poll reveals that for day-to-day risk management the use of one-day VaR is universal among banks surveyed. However, for internal capital adequacy and strategic risk management, banks are generally moving beyond short-horizon models (e.g. one-day and 10-day VaR). It is now acknowledged that, to determine the level of capital necessary to remain in business after sustaining a large loss, risk must be assessed over a longer period. Shorter horizons do not address the liquidity risk for all exposures and do not capture tail events that are important for capital adequacy. Further, almost all banks' VaR models capture non-linearities at a local level (i.e. small price changes) for much of their market risk exposure, but many banks' VaR models fail to capture non-linearity at a global level (i.e., large price changes). A common weakness in the capture of non-linearity is the use of scaling of one-day VaR to estimate exposures at longer holding periods. Such scaling only captures local non-linearity in the range of one-day price changes and can underestimate non-linear exposure over longer horizons. The Committee has agreed that the differentiation of market liquidity across the trading book will be based on the concept of *liquidity horizons*[1]. It proposes that banks' trading book exposures be assigned to a small number of liquidity horizon categories ranging from ten days to one year. The shortest liquidity horizon (most liquid exposures) is in line with the current 10-day VaR treatment in the trading book. The longest liquidity horizon (least liquid exposures) matches the banking book horizon at one year.

The estimation of the ES for several trading desks and taking into account different liquidity horizons is computationally very involved. In this work we present efficient and robust numerical techniques to address the aforementioned challenges. We compute the VaR and ES risk measures of a market portfolio and we assume that the holding period follows a certain positive stochastic process to account for liquidity risk. We will therefore measure the risk in the situation where the holding period is the liquidity horizon, and we will use these two terms interchangeably throughout the paper. While the regulatory capital calculation is based on a series of increasing deterministic liquidity horizons for different assets in the trading book, our approach does not distinguish between asset classes and is therefore more suitable for an internal risk management assessment. To our best knowledge, this idea was first introduced in [6] as a proposal to open a research effort in stochastic holding period models for risk measures. In that paper the authors assume that the log-return on the portfolio value is normally distributed, which facilitates the calculation of the risk measures. Within this work, we go a step further by considering more realistic models for the log-value of the portfolio. On the one hand we propose the use of the delta-gamma approach [19], where it is assumed that the change in portfolio value is a quadratic function of the changes in the risk factors. On the other hand, we consider the Merton jump diffusion (MJD) model [18] and the Kou model [14] to drive the log-return on the portfolio value. Under any of these scenarios, the closed formulae to compute the risk measures within the Gaussian setting in [6] are not available anymore. However, the characteristic function[2] of the change in (log-)value of the portfolio is known in closed form for most of the interesting processes in finance, in particular for the two models mentioned above. We therefore recover the density function from its Fourier transform and then we calculate the VaR and the ES values. Among the methods available in the literature for Fourier inversion, we choose the SWIFT method originally developed in [21] for option pricing, where the density function is approximated by a finite combination of Shannon wavelets. A Haar wavelets-based procedure as well as a cosine series expansion have been previously used in the literature in [20]

[1]The definition of liquidity horizon given in [5] is: *"the time required to exit or hedge a risk position without materially affecting market prices in stressed market conditions."*

[2]We define the characteristic function of a random variable X as the Fourier transform of its density function f_X, i.e. $\hat{f}_X(u) = \int_{\mathbb{R}} e^{-iux} f_X(x)dx$.

to recover the density function within the delta-gamma approach with the multivariate Gaussian model for the individual risk factors. The most important feature of the present method is that the scale of approximation is estimated a priori by means of the characteristic function, and this makes this method a real applicable one in practice, as opposed to the aforementioned numerical methods based on trial and error.

The layout of the paper is as follows. We define the risk measures and introduce the concept of stochastic liquidity horizon (SLH) in Section 1.1. In Section 2, we give a brief overview about Shannon wavelets theory and recall the details on the SWIFT method. Section 3 is devoted to explaining the methodology to calculate the VaR and ES risk measures. A complete error analysis is presented in Section 4 as well as the way to select the parameters of the numerical method. A wide variety of examples is given in Section 5, and finally Section 6 concludes.

1.1. **Risk measures and stochastic liquidity horizon.** We build upon the work in [6] and devote this section to provide the mathematical framework and basic definitions that we will use in subsequent sections.

Let us assume that the liquidity horizon follows a certain stochastic process $\{H(t)\}_{t\geq 0}$ where $H(t)$ is a positive random variable associated to the liquidity horizon at time $t \geq 0$. Let $V(t)$ be the value of the portfolio under consideration at time t. We are interested in measuring the change in value of the portfolio within the SLH framework. To do this, we consider two different approaches. The first one is the well-known delta-gamma approximation [19], which assumes that the change in value of the portfolio is a quadratic function of the change in value of the risk factors. We recently proposed an efficient numerical method to compute the VaR and ES with a deterministic holding period (see [20] for details). Within the present context of stochastic liquidity horizon, the change in value of the portfolio under the delta-gamma approach is defined as $\Delta V := V(t + H(t)) - V(t)$. To our best knowledge, this is the first time that the delta-gamma approach is considered with a stochastic holding period. The second approach consists of assuming that the value of the portfolio follows a certain stochastic process and we are therefore interested in measuring the change in the log-value of the portfolio rather than in the value itself. Then, we define $X := \ln(V(t + H(t))) - \ln(V(t))$. Let $f_{\Delta V}$ (respectively f_X) be the probability density function (PDF) of ΔV (respectively X) and $F_{\Delta V}$ (respectively F_X) its cumulative distribution function (CDF). If we assume that we short the portfolio, then the right tail of f_X represents losses. Given some confidence level $\alpha \in (0, 1)$, the VaR to measure the risk of holding the portfolio during the stochastic period $H(t)$ is given by the smallest number l such that the probability that the loss X exceeds l is no larger than $1 - \alpha$, where typically $\alpha \geq 0.95$. Formally,

$$\mathrm{VaR}(\alpha) := \inf\{l \in \mathbb{R} : \mathbb{P}(X > l) \leq 1 - \alpha\} = \inf\{l \in \mathbb{R} : F_X(l) \geq \alpha\}. \tag{1}$$

By definition, ES is related to VaR by,

$$\mathrm{ES}(\alpha) := \frac{1}{1-\alpha}\int_\alpha^1 \mathrm{VaR}(u)\, du.$$

Instead of fixing a particular level α, we average VaR over all levels $u \geq \alpha$ and thus, as pointed out in [17], we "look further into the tail" of the loss distribution. Obviously, $\mathrm{ES}(\alpha)$ depends only on the distribution of X, and $\mathrm{ES}(\alpha) \geq \mathrm{VaR}(\alpha)$. For continuous loss distributions an even more intuitive expression can be derived that shows that ES can be interpreted as the expected loss that is incurred in the event that VaR is exceeded. For an integrable loss X with continuous distribution function F_X and for any $\alpha \in (0, 1)$ we have,

$$\mathrm{ES}(\alpha) = \mathbb{E}(X | X \geq \mathrm{VaR}(\alpha)),$$

or, in integral form,

$$\mathrm{ES}(\alpha) = \frac{1}{1-\alpha}\int_{\mathrm{VaR}(\alpha)}^{+\infty} x f_X(x)\, dx. \tag{2}$$

Note that when we work under the delta-gamma approach, then we replace X, F_X, f_X by $\Delta V, F_{\Delta V}, f_{\Delta V}$ in (1) and (2). It is worth remarking that ES is a coherent measure of risk, satisfying in particular, the axiom of sub-additivity in line with the concept of diversification. For more details we refer the reader to [1] and [17].

In practice, analytical expressions are not available, and Monte Carlo (MC) simulation is often used to compute the risk measures, being the main drawback the computational effort. From this point of view, the situation worsens when we consider a stochastic liquidity horizon $H(t)$, since an extra source of randomness is introduced and must be simulated as well. For this reason, there is an increasing interest in looking for alternative and more efficient methods. Here we propose the SWIFT method, which was originally developed for European options pricing in [21] and further extended to price Bermuda options ([15]), European options under high dimensional stochastic models ([10]) and two-dimensional options ([8]). The SWIFT method gives us an accurate and extremely fast recovery of the density function and we give a prescription on how to select the parameters appearing in the numerical method. All these features make our proposal efficient, robust and reliable for practical implementation.

2. Shannon wavelets and SWIFT method

In this section we give a brief review on the SWIFT method [21], since this is the method that we have selected to carry out the computation of the risk measures. For sake of completeness we devote a section to the basic theory on Shannon wavelets.

2.1. Multi-resolution analysis and Shannon wavelets.

Consider the space of square-integrable functions, denoted by $L^2(\mathbb{R})$, where,

$$L^2(\mathbb{R}) = \left\{ f : \int_{-\infty}^{+\infty} |f(x)|^2 \,\mathrm{d}x < \infty \right\}.$$

A general structure for wavelets in $L^2(\mathbb{R})$ is called a *multi-resolution analysis*. We start with a family of closed nested subspaces in $L^2(\mathbb{R})$,

$$\ldots \subset \mathcal{V}_{-2} \subset \mathcal{V}_{-1} \subset \mathcal{V}_0 \subset \mathcal{V}_1 \subset \mathcal{V}_2 \subset \ldots,$$

where,

$$\bigcap_{m\in\mathbb{Z}} \mathcal{V}_m = \{0\} \ , \qquad \overline{\bigcup_{m\in\mathbb{Z}} \mathcal{V}_m} = L^2(\mathbb{R}) \ ,$$

and,

$$f(x) \in \mathcal{V}_m \Longleftrightarrow f(2x) \in \mathcal{V}_{m+1}.$$

If these conditions are met, then there exists a function $\varphi \in \mathcal{V}_0$ that generates an orthonormal basis, denoted by $\{\varphi_{m,k}\}_{k\in\mathbb{Z}}$, for each $\mathcal{V}_m$ subspace, where,

$$\varphi_{m,k}(x) = 2^{m/2}\varphi(2^m x - k).$$

The function φ is usually referred to as the *scaling function* or *father wavelet*.

For any $f \in L^2(\mathbb{R})$, a projection map of $L^2(\mathbb{R})$ onto $\mathcal{V}_m$, denoted by $\mathcal{P}_m : L^2(\mathbb{R}) \to \mathcal{V}_m$, is defined by means of,

$$\mathcal{P}_m f(x) = \sum_{k\in\mathbb{Z}} c_{m,k}\varphi_{m,k}(x). \tag{3}$$

Here,

$$c_{m,k} = \langle f, \varphi_{m,k} \rangle \ , \tag{4}$$

where $< f, g >:= \int_{\mathbb{R}} f(x)\overline{g}(x) \,\mathrm{d}x$ denotes the inner product in $L^2(\mathbb{R})$, with $\overline{g}$ being the complex conjugate of g.

Considering higher m values (i.e. when more terms are used), the truncated series representation of the function f improves. As opposed to Fourier series, a key fact regarding the use of wavelets is that wavelets can be moved (by means of the k value), stretched or compressed (by means of the m value) to accurately represent the local properties of a function. A basic reference on wavelets is [11].

In this paper, we employ Shannon wavelets [7]. A set of Shannon scaling functions $\varphi_{m,k}$ in the subspace $\mathcal{V}_m$ is defined as,

$$\varphi_{m,k}(x) = 2^{m/2}\frac{\sin(\pi(2^m x - k))}{\pi(2^m x - k)} = 2^{m/2}\varphi(2^m x - k), \quad k \in \mathbb{Z}, \tag{5}$$

where,

$$\varphi(x) = \mathrm{sinc}(x) = \begin{cases} \dfrac{\sin(\pi x)}{\pi x} & \text{if } x \neq 0, \\ 1 & \text{if } x = 0, \end{cases} \tag{6}$$

is the basic (Shannon) scaling function.

2.2. **SWIFT method.** Given a function $f \in L^2(\mathbb{R})$, we consider its expansion in terms of Shannon scaling functions at the level of resolution m. Our aim is to recover the coefficients $c_{m,k}$ of this approximation from the Fourier transform of the function f, denoted by $\hat{f}$, which is assumed to be known in closed-form. Here,

$$\hat{f}(\xi) = \int_{\mathbb{R}} e^{-i\xi x} f(x)\,\mathrm{d}x\ . \tag{7}$$

The SWIFT method [21] can effectively achieve this purpose. In the present context, the SWIFT method is used to obtain an approximation of the density function of the random variable associated to the change in value (or log-value) of a certain portfolio within a period of time, as introduced in Section 1.1.

Following wavelets theory, a function $f \in L^2(\mathbb{R})$ can be approximated at the level of resolution m by,

$$f(x) \approx \mathcal{P}_m f(x) = \sum_{k\in\mathbb{Z}} c_{m,k}\varphi_{m,k}(x), \tag{8}$$

where $\mathcal{P}_m f$ converges to f in $L^2(\mathbb{R})$, i.e. $\|f - \mathcal{P}_m f\|_2 \to 0$, when $m \to +\infty$. Here, the coefficients $c_{m,k}$ and the scaling functions $\varphi_{m,k}$ are defined in (4) and (5), respectively.

The infinite series in (8) is well-approximated (see Lemma 1 of [21] for details) by a finite summation without loss of considerable density mass,

$$\mathcal{P}_m f(x) \approx f_m(x) := \sum_{k=k_1}^{k_2} c_{m,k}\varphi_{m,k}(x), \tag{9}$$

for certain accurately chosen values k_1 and k_2.

The next step is the computation of the coefficients in (9). Recalling (4) and (5), we have that,

$$c_{m,k} = \langle f, \varphi_{m,k}\rangle = \int_{\mathbb{R}} f(x)\overline{\varphi}_{m,k}(x)\,\mathrm{d}x = 2^{m/2}\int_{\mathbb{R}} f(x)\varphi(2^m x - k)\mathrm{d}x. \tag{10}$$

Using the classical Vieta's formula [12], the cardinal sine can be expressed as the following infinite product,

$$\varphi(t) = \mathrm{sinc}(t) = \prod_{j=1}^{+\infty}\cos\left(\frac{\pi t}{2^j}\right)\ . \tag{11}$$

If we truncate the infinite product (11) to a finite product with a total of J terms, then, thanks to the cosine product-to-sum identity [22], we have

$$\prod_{j=1}^{J}\cos\left(\frac{\pi t}{2^j}\right) = \frac{1}{2^{J-1}}\sum_{j=1}^{2^{J-1}}\cos\left(\frac{2j-1}{2^J}\pi t\right). \tag{12}$$

By (11) and (12) the sinc function can thus be approximated as,

$$\varphi(t) = \mathrm{sinc}(t) \approx \mathrm{sinc}^*(t) := \frac{1}{2^{J-1}}\sum_{j=1}^{2^{J-1}}\cos\left(\frac{2j-1}{2^J}\pi t\right). \tag{13}$$

Replacing the function φ in (10) by the approximation (13) we obtain,

$$c_{m,k} \approx c^*_{m,k} := \frac{2^{m/2}}{2^{J-1}} \sum_{j=1}^{2^{J-1}} \int_{\mathbb{R}} f(x) \cos\left(\frac{2j-1}{2^J}\pi(2^m x - k)\right) \mathrm{d}x. \tag{14}$$

Next, by taking into account that $\Re\left(\hat{f}(\xi)\right) = \int_{\mathbb{R}} f(x)\cos(\xi x)\,\mathrm{d}x$ in (7), where $\Re(z)$ denotes the real part of z, and observing that,

$$\hat{f}(\xi) e^{ik\pi\frac{2j-1}{2^J}} = \int_{\mathbb{R}} e^{-i\left(\xi x - \frac{k\pi(2j-1)}{2^J}\right)} f(x)\mathrm{d}x,$$

we can simplify (14) to,

$$c_{m,k} \approx c^*_{m,k} = \frac{2^{m/2}}{2^{J-1}} \sum_{j=1}^{2^{J-1}} \Re\left[\hat{f}\left(\frac{(2j-1)\pi 2^m}{2^J}\right) e^{\frac{ik\pi(2j-1)}{2^J}}\right]. \tag{15}$$

Putting everything together gives the following approximation of f,

$$f(x) \approx f^*_m(x) := \sum_{k=k_1}^{k_2} c^*_{m,k}\varphi_{m,k}(x), \tag{16}$$

where $\varphi_{m,k}$ and $c^*_{m,k}$ are defined in (5) and (15), respectively.

Remark 1. *Formula (15) can be conveniently rearranged to compute the coefficients with the use of the fast Fourier transform (FFT). We will give a review on the use of the FFT in this context in Section 4, along with the way to select the parameters m and J in (15) and k_1, k_2 in (16).*

3. Risk Measures

In this section we present formulae to calculate the VaR and ES risk measures. The strategy that we follow consists of recovering the density function of the change in value (or log-value) of a certain portfolio from its Fourier transform, which is known in many situations of interest. To simplify the notation, we assume along the present section that f is the unknown density function while $\hat{f}$ is its known Fourier transform. Let us assume that f is well approximated at scale of resolution m in a finite interval $[a, b] \subset \mathbb{R}$. We define $k_1 := \lfloor 2^m a \rfloor$ and $k_2 := \lceil 2^m b \rceil$, where $\lfloor x \rfloor$ denotes the greatest integer less than or equal to x, and $\lceil x \rceil$ denotes the smallest integer greater than or equal to x. In Section 4 we give an explanation on the selection of the scale and the interval of approximation as well as the algorithm to get the VaR and ES values.

3.1. Value-at-Risk.

From the definition of VaR in (1) we have to compute the value $l_\alpha := \mathrm{VaR}(\alpha)$, with $a < l_\alpha < b$ such that $I - \alpha = 0$, where,

$$I := \int_{-\infty}^{l_\alpha} f(x)dx. \tag{17}$$

We truncate the infinite integration domain $(-\infty, l_\alpha]$ in (17) into a finite domain $[a, l_\alpha]$,

$$I_1 := \int_{a}^{l_\alpha} f(x)dx, \tag{18}$$

and we replace f in (18) by its approximation f^*_m in terms of Shannon scaling wavelets as in (16), this is,

$$I^*_m := \int_a^{l_\alpha} f^*_m(x)dx = \sum_{k=k_1}^{k_2} c^*_{m,k} \int_a^{l_\alpha} \varphi_{m,k}(x)dx = 2^{m/2} \sum_{k=k_1}^{k_2} c^*_{m,k} \int_a^{l_\alpha} \mathrm{sinc}(2^m x - k)dx. \tag{19}$$

Now, if we make the change of variables $y = 2^m x - k$ and replace sinc by its approximation sinc* in (13), we end up with the expression,

(20)

$$\begin{aligned} I_m^*(J) :&= \frac{1}{2^{m/2}} \frac{1}{2^{J-1}} \sum_{k=k_1}^{k_2} c_{m,k}^* \sum_{j=1}^{2^{J-1}} \int_{2^m a - k}^{2^m l_\alpha - k} \cos\left(\frac{2j-1}{2^J}\pi y\right) dy \\ &= \frac{2}{\pi} \frac{1}{2^{m/2}} \sum_{k=k_1}^{k_2} c_{m,k}^* \sum_{j=1}^{2^{J-1}} \frac{1}{2j-1} \left[\sin\left(\frac{2j-1}{2^J}\pi(2^m l_\alpha - k)\right) - \sin\left(\frac{2j-1}{2^J}\pi(2^m a - k)\right) \right]. \end{aligned}$$

Finally, we use a root-finding method to determine the value l_α such that $I_m^*(J) - \alpha = 0$ and we call it VaR$^*(\alpha)$.

Remark 2. *We see that the area underneath f is tightly related to the computation of the density coefficients $c_{m,k}^*$ in (15), and we provide an alternative method to calculate the VaR. Although this method is extremely fast in terms of CPU time, we perform all the numerical experiments with the method presented above since it is more accurate and keeps a good balance between CPU time and accuracy. We define,*

$$I_1(m,h) := \int_{-\infty}^{h/2^m} f(x)dx, \tag{21}$$

where $h \in \mathbb{Z}$, and we truncate the infinite integration domain $(-\infty, h/2^m]$ into a finite domain $[k_1/2^m, h/2^m]$,

$$I_1(m,h) \approx I_2(m,h) := \int_{\frac{k_1}{2^m}}^{\frac{h}{2^m}} f(x)dx. \tag{22}$$

If we apply the trapezoidal rule with step $1/2^m$, then we end up with the following formula,

$$I_2(m,h) \approx S_1(m,h) := \frac{1}{2^{m+1}} \left[2 \sum_{k=k_1+1}^{h-1} f\left(\frac{k}{2^m}\right) + f\left(\frac{k_1}{2^m}\right) + f\left(\frac{h}{2^m}\right) \right]. \tag{23}$$

From (5) and (9) we have that $f\left(\frac{l}{2^m}\right) \approx 2^{m/2} c_{m,l}$, for all $l \in \mathbb{Z}$, and therefore, applying this to the expression (23) gives us,

$$\begin{aligned} S_1(m,h) \approx S_2(m,h) :&= \frac{1}{2^{m+1}} \left[2^{m/2+1} \sum_{k=k_1+1}^{h-1} c_{m,k} + 2^{m/2} c_{m,k_1} + 2^{m/2} c_{m,h} \right] \\ &= \frac{1}{2^{m/2}} \left[\frac{c_{m,k_1}}{2} + \sum_{k=k_1+1}^{h-1} c_{m,k} + \frac{c_{m,h}}{2} \right]. \end{aligned} \tag{24}$$

Finally, the coefficients $c_{m,k}$ in (24) are approximated by $c_{m,k}^*$ in expression (15). Then,

$$S_2(m,h) \approx S_3(m,h) := \frac{1}{2^{m/2}} \left[\frac{c_{m,k_1}^*}{2} + \sum_{k=k_1+1}^{h-1} c_{m,k}^* + \frac{c_{m,h}^*}{2} \right]. \tag{25}$$

Note that the VaR can be calculated just by adding density coefficients until the value of $S_3(m,h)$ reaches (or is approximately equal to) the confidence level α. We add terms until the condition $S_3(m,h^*) \leq \alpha \leq S_3(m,h^*+1)$ is satisfied for a certain $h^* \in \mathbb{Z}$ and we select the VaR value as the midpoint of the interval $[\frac{h^*}{2^m}, \frac{h^*+1}{2^m}]$, this is,

$$\widetilde{VaR}(\alpha) := \frac{2h^*+1}{2^{m+1}}. \tag{26}$$

3.2. **Expected Shortfall.** The ES can be determined once we obtain the VaR value as detailed in Section 3.1. From (2), we have to compute the integral,

$$\mathrm{ES}(\alpha) = \frac{1}{1-\alpha}\int_{l_\alpha}^{+\infty} x f(x)\, dx. \tag{27}$$

We replace l_α by the VaR value computed in the previous section, and we define $l_\alpha^* := \mathrm{VaR}^*(\alpha)$. Now, we focus on the calculation of the following integral,

$$\mathrm{ES}_1(\alpha) := \frac{1}{1-\alpha}\int_{l_\alpha^*}^{+\infty} x f(x)\, dx, \tag{28}$$

and truncate the infinite integration domain $[l_\alpha^*, +\infty)$ into the finite domain $[l_\alpha^*, b]$, this gives us,

$$\mathrm{ES}_2(\alpha) := \frac{1}{1-\alpha}\int_{l_\alpha^*}^{b} x f(x)\, dx. \tag{29}$$

The last step consists of replacing the function f in (29) by its approximation f_m^*, and making the change of variables $y = 2^m x - k$, we obtain,

$$\begin{aligned}
\mathrm{ES}_m^*(\alpha) :&= \frac{1}{1-\alpha}\int_{l_\alpha^*}^{b} x f_m^*(x)\, dx = \frac{2^{m/2}}{1-\alpha}\sum_{k=k_1}^{k_2} c_{m,k}^* \int_{l_\alpha^*}^{b} x \frac{\sin\left(\left(2^m x - k\right)\pi\right)}{\left(2^m x - k\right)\pi} dx \\
&= \frac{2^{\frac{m}{2}}}{(1-\alpha)\, 2^{2m}} \sum_{k=k_1}^{k_2} c_{m,k}^* \int_{2^m l_\alpha^* - k}^{2^m b - k} (y+k)\,\frac{\sin(\pi y)}{\pi y} dy \\
&= \frac{1}{(1-\alpha)\, 2^{\frac{3}{2}m}} \sum_{k=k_1}^{k_2} c_{m,k}^* \left[\frac{1}{\pi}\int_{2^m l_\alpha^* - k}^{2^m b - k} \sin(\pi y)\, dy + k\int_{2^m l_\alpha^* - k}^{2^m b - k} \mathrm{sinc}(y) dy\right].
\end{aligned} \tag{30}$$

The first integral of the right hand side in (30) is solved analytically,

$$\int_{2^m l_\alpha^* - k}^{2^m b - k} \sin(\pi y)\, dt = \frac{1}{\pi}\left[\cos\left(\pi\left(2^m l_\alpha^* - k\right)\right) - \cos\left(\pi\left(2^m b - k\right)\right)\right], \tag{31}$$

while for the second integral $\mathcal{I} := \int_{2^m l_\alpha^* - k}^{2^m b - k} \mathrm{sinc}(y) dy$ we use the formula in (13) to approximate the cardinal sine function and $\mathcal{I}$ can be replaced by,

$$\begin{aligned}
\mathcal{I}_1 :&= \frac{1}{2^{J-1}}\int_{2^m l_\alpha^* - k}^{2^m b - k} \sum_{j=1}^{2^{J-1}} \cos\left(\frac{2j-1}{2^J}\pi y\right) dy = \frac{1}{2^{J-1}} \sum_{j=1}^{2^{J-1}} \int_{2^m l_\alpha^* - k}^{2^m b - k} \cos\left(\frac{2j-1}{2^J}\pi y\right) dy \\
&= \frac{2}{\pi}\sum_{j=1}^{2^{J-1}} \frac{1}{(2j-1)}\left[\sin\left(\frac{2j-1}{2^J}\pi\left(2^m b - k\right)\right) - \sin\left(\frac{2j-1}{2^J}\pi\left(2^m l_\alpha^* - k\right)\right)\right].
\end{aligned} \tag{32}$$

Finally, by (30), (31) and (32), the Expected Shortfall $\mathrm{ES}(\alpha)$ can be calculated with the formula,

$$\begin{aligned}
\mathrm{ES}^*(\alpha) :&= \frac{1}{(1-\alpha)\, 2^{\frac{3}{2}m}} \sum_{k=k_1}^{k_2} c_{m,k}^* \left[\frac{1}{\pi^2}\left(\cos\left(\pi\left(2^m l_\alpha^* - k\right)\right) - \cos\left(\pi\left(2^m b - k\right)\right)\right)\right. \\
&\left. + \frac{2}{\pi} k \sum_{j=1}^{2^{J-1}} \frac{1}{(2j-1)}\left(\sin\left(\frac{2j-1}{2^J}\pi\left(2^m b - k\right)\right) - \sin\left(\frac{2j-1}{2^J}\pi\left(2^m l_\alpha^* - k\right)\right)\right)\right].
\end{aligned} \tag{33}$$

Remark 3. *Note that we can speed up the evaluation of (20) and (33) by means of a discrete sine transform.*

4. Error analysis and selection of parameters

In this section we perform an error analysis on the SWIFT method when it is used to calculate the risk measures, and explain how to determine the value of the parameters that intervene in the numerical method.

4.1. **Error estimation in the computation of VaR.** Let us define $\mathcal{E} := |I - I^*_m(J)|$, $\mathcal{E}_1 := |I - I_1|$, $\mathcal{E}_2 := |I_1 - I^*_m|$ and $\mathcal{E}_3 := |I^*_m - I^*_m(J)|$. Then, the overall error when approximating I in (17) by $I^*_m(J)$ in (20) can be bounded by,

$$\mathcal{E} \leq \mathcal{E}_1 + \mathcal{E}_2 + \mathcal{E}_3. \tag{34}$$

From (17) and (18) we have,

$$\mathcal{E}_1 \leq \int_{-\infty}^{a} f(x)dx. \tag{35}$$

We can make this integral arbitrarily small by selecting a appropriately, since f is a density function.

We define the projection error, denoted by ϵ_p, as,

$$\epsilon_p := |f(x) - \mathcal{P}_m f(x)| = |f(x) - \sum_{k \in \mathbb{Z}} c_{m,k}\varphi_{m,k}(x)| \ . \tag{36}$$

We also define the truncation error, denoted by ϵ_t, as,

$$\epsilon_t := |\mathcal{P}_m f(x) - f_m(x)| = |\sum_{k \notin \{k_1,\ldots,k_2\}} c_{m,k}\varphi_{m,k}(x)| \ .$$

We denote by ϵ_c the error arising from using approximated coefficients $c^*_{m,k}$ instead of the exact ones $c_{m,k}$. We have,

$$\epsilon_c := |f_m(x) - f^*_m(x)| = |\sum_{k=k_1}^{k_2} (c_{m,k} - c^*_{m,k})\varphi_{m,k}(x)|.$$

Then, we have,

$$|f(x) - f^*_m(x)| \leq \epsilon_p + \epsilon_t + \epsilon_c \ , \tag{37}$$

and,

$$\mathcal{E}_2 \leq \int_a^{l_\alpha} |f(x) - f^*_m(x)|dx \leq (l_\alpha - a)(\epsilon_p + \epsilon_t + \epsilon_c) \leq (b - a)(\epsilon_p + \epsilon_t + \epsilon_c). \tag{38}$$

First, we consider the projection error ϵ_p. The projection $\mathcal{P}_m f$ can be written as [15],

$$\mathcal{P}_m f(x) = \frac{1}{2\pi}\int_{-2^m\pi}^{2^m\pi} \hat{f}(\xi)e^{i\xi x}\mathrm{d}\xi \ . \tag{39}$$

By definition of the inverse Fourier transform of f, we have,

$$f(x) = \frac{1}{2\pi}\int_{\mathbb{R}} \hat{f}(\xi)e^{i\xi x}\mathrm{d}\xi \ . \tag{40}$$

Let,

$$K(v) = \frac{1}{2\pi}\int_{|\xi|>v} |\hat{f}(\xi)|\mathrm{d}\xi \ , \tag{41}$$

then,

$$\epsilon_p \leq K(2^m\pi) \ . \tag{42}$$

Next, we consider the truncation error ϵ_t. We observe that,

$$\epsilon_t = |\mathcal{P}_m f(x) - f_m(x)| \leq 2^{m/2} \sum_{k \notin \{k_1,\ldots,k_2\}} |c_{m,k}| \ . \tag{43}$$

since $|\varphi_{m,k}(x)| \leq 2^{m/2}$. The following theorem allows us to give an estimation of the size of the coefficients $c_{m,k}$ in terms of the rate of decay of the density function f.

Theorem 1 (Theorem 1.3.2 of [23]). *Let f be defined on $\mathbb{R}$, and let $\hat{f}$ be its Fourier transform such that for some positive constant d,*

$$|\hat{f}(y)| = \mathcal{O}\left(e^{-d|y|}\right), \quad |y| \to \pm\infty. \tag{44}$$

Then, as $h \to 0$,

$$\frac{1}{h}\int_{\mathbb{R}} f(t)S(j,h)(t)dt - f(jh) = \mathcal{O}\left(e^{-\frac{\pi d}{h}}\right), \tag{45}$$

where $S(j,h)(t) := sinc\left(\frac{x}{h} - j\right)$.

If we consider $h = \frac{1}{2^m}$, then by Theorem 1, the terms $|c_{m,k}|$ can be well approximated by $\frac{1}{2^{m/2}} f\left(\frac{k}{2^m}\right)$ provided that $|\hat{f}|$ decays like in (44). As pointed out in [15], this rate of decay is typically encountered in most of the interesting processes in finance, like for instance the GBM, MJD and Kou models, to name just a few. Then, we can assume a certain rate of decay for f to conclude that the series in (43) is a convergent series of terms which decrease very fast in value when k goes to minus and plus infinity.

Finally, we consider ϵ_c. The coefficients $c_{m,k}$ are to be calculated by means of Vieta's formula and the numerical error can be estimated as,

$$\epsilon_c \leq \sum_{k=k_1}^{k_2} |c_{m,k} - c^*_{m,k}||\varphi_{m,k}(x)| \leq 2^{m/2} \sum_{k=k_1}^{k_2} |c_{m,k} - c^*_{m,k}| \ . \tag{46}$$

The coefficients approximation error is studied in Theorem 1 of [21] and it states the following theorem.

Theorem 2 (Theorem 1 of [21]). *Let $F(x)$ be the distribution function of a random variable X and define $H(x) := F(-x) + 1 - F(x)$. Let $\mathcal{A} > 0$ be a constant such that $H(\mathcal{A}) < \epsilon$, for $\epsilon > 0$. Define $M_{m,k} := \max\left(|2^m\mathcal{A} - k|, |2^m\mathcal{A} + k|\right)$ and consider $J \geq \log_2\left(\pi M_{m,k}\right)$. Then,*

$$|c_{m,k} - c^*_{m,k}| \leq 2^{m/2}\left(2\epsilon + \sqrt{2\mathcal{A}}\|f\|_2 \frac{\left(\pi M_{m,k}\right)^2}{2^{2(J+1)} - \left(\pi M_{m,k}\right)^2}\right), \tag{47}$$

and $\lim_{J\to+\infty} c^*_{m,k} = c_{m,k}$.

If we define $\mathcal{A} := \max(|a|, |b|)$ and assume that $H(\mathcal{A}) < \epsilon$, then we can apply Theorem 2 with $\jmath \geq \log_2(\pi M_m)$, where $M_m := \max_{k_1<k<k_2} M_{m,k}$. Finally,

$$\epsilon_c \leq 2^{m/2}\sum_{k=k_1}^{k_2} |c_{m,k} - c^*_{m,k}| \leq 2^m(k_2 - k_1 + 1)\left(2\epsilon + \sqrt{2\mathcal{A}}\|f\|_2 \frac{(\pi M_m)^2}{2^{2(\jmath+1)} - (\pi M_m)^2}\right). \tag{48}$$

Next we consider,

$$\mathcal{E}_3 := |I^*_m - I^*_m(J)| \leq 2^{m/2}\sum_{k=k_1}^{k_2} |c^*_{m,k}| \int_a^{l_\alpha} |\mathrm{sinc}(2^m x - k) - \mathrm{sinc}^*(2^m x - k)|dx. \tag{49}$$

If we make the change of variables $y = 2^m x - k$, then,

$$\mathcal{E}_3 \leq \frac{1}{2^{m/2}}\sum_{k=k_1}^{k_2} |c^*_{m,k}| \int_{2^m a-k}^{2ml_\alpha - k} |\mathrm{sinc}(y) - \mathrm{sinc}^*(y)|dy. \tag{50}$$

We observe from (14) that $|c^*_{m,k}| \leq 2^{m/2}$. Further, we will use the following lemma to get an upper bound of the integral in (50).

Lemma 1 (Lemma 2 of [21]). *Define the absolute error $\mathcal{E}_V(t) := sinc(t) - sinc^*(t)$. Then,*

$$|\mathcal{E}_V(t)| \leq \frac{(\pi c)^2}{2^{2(J+1)} - (\pi c)^2},$$

for $t \in [-c, c]$, where $c \in \mathbb{R}, c > 0$ and $J \geq \log_2(\pi c)$.

Since $-2^m\mathcal{A}-k \leq 2^m a - k \leq y \leq 2^m l_\alpha - k \leq 2^m\mathcal{A}-k$, then from (50) and Lemma 1 we have,

$$\int_{2^m a-k}^{2^m l_\alpha - k} |\mathrm{sinc}(y)-\mathrm{sinc}^*(y)|dy \leq \int_{-M_m}^{M_m} |\mathrm{sinc}(y)-\mathrm{sinc}^*(y)|dy \leq \frac{2\pi^2 (M_m)^3}{2^{2(J+1)}-(\pi M_m)^2}. \tag{51}$$

Finally,

$$\mathcal{E}_3 \leq (k_2-k_1+1)\frac{2\pi^2 (M_m)^3}{2^{2(J+1)}-(\pi M_m)^2}. \tag{52}$$

4.2. **Error estimation in the computation of ES.** Let us define $\bar{\mathcal{E}} := |\mathrm{ES}_1(\alpha)-\mathrm{ES}^*(\alpha)|$, $\bar{\mathcal{E}}_1 := |\mathrm{ES}_1(\alpha)-\mathrm{ES}_2(\alpha)|$, $\bar{\mathcal{E}}_2 := |\mathrm{ES}_2(\alpha)-\mathrm{ES}^*_m(\alpha)|$ and $\bar{\mathcal{E}}_3 := |\mathrm{ES}^*_m(\alpha)-\mathrm{ES}^*(\alpha)|$. Then, the overall error when approximating $\mathrm{ES}_1(\alpha)$ in (28) by $\mathrm{ES}^*(\alpha)$ in (33) is bounded by,

$$\bar{\mathcal{E}} \leq \bar{\mathcal{E}}_1+\bar{\mathcal{E}}_2+\bar{\mathcal{E}}_3. \tag{53}$$

The error $\bar{\mathcal{E}}_1$ can be bounded following an analogous argument as in Section 4.1. Let us study $\bar{\mathcal{E}}_2$ in detail,

$$\bar{\mathcal{E}}_2 = |\mathrm{ES}_2(\alpha)-\mathrm{ES}^*_m(\alpha)| = \left|\frac{1}{1-\alpha}\int_{l^*_\alpha}^{b} x\left(f(x)-f^*_m(x)\right)dx\right| \leq \frac{1}{1-\alpha}\int_{l^*_\alpha}^{b} x\left|f(x)-f^*_m(x)\right|dx. \tag{54}$$

Then, from (37) we have,

$$\bar{\mathcal{E}}_2 \leq \left[\frac{1}{1-\alpha}\int_{l^*_\alpha}^{b} x\,dx\right](\epsilon_p+\epsilon_t+\epsilon_c) = \frac{b^2-(l^*_\alpha)^2}{2(1-\alpha)}(\epsilon_p+\epsilon_t+\epsilon_c). \tag{55}$$

Regarding $\bar{\mathcal{E}}_3$, we observe that the source of error is the replacement of sinc by sinc* in $\mathcal{I} := \int_{2^m l^*_\alpha - k}^{2^m b-k}\mathrm{sinc}(y)dy$. Thus, we can consider a similar argument as in the last part of Section 4.1 to get the same bound given in (51) for the error $|\mathcal{I}-\mathcal{I}_1|$.

4.3. **Choice of m, J and the truncation interval $[a,b]$.** Looking at expressions (20) and (33) for computing the VaR and ES values respectively, we can observe that the parameters m and J must be selected before we carry out the approximation. As we have shown in Section 4.1, the projection error (36) is bounded by,

$$\epsilon_p \leq K(2^m\pi), \tag{56}$$

where,

$$K(v) = \frac{1}{2\pi}\int_{|\xi|>v}|\hat{f}(\xi)|\mathrm{d}\xi. \tag{57}$$

In our setting, the characteristic function $\hat{f}$ is known in closed form and we can therefore calculate the value of m that makes the projection error smaller than a certain tolerance ϵ_m. In general, the integral in (57) cannot be solved analytically and we compute the value of m that satisfies,

$$\frac{1}{2\pi}\left(|\hat{f}(-2^m\pi)|+|\hat{f}(2^m\pi)|\right) \leq \epsilon_m. \tag{58}$$

Note that a more accurate method can be used to compute the integral in (57) based on numerical integration. Moreover, we can make a more conservative selection of the scale m, when computing the ES, by considering the error amplifying factor $1/(1-\alpha)$ in (55), this is,

$$\frac{1}{1-\alpha}\cdot\frac{1}{2\pi}\left(|\hat{f}(-2^m\pi)|+|\hat{f}(2^m\pi)|\right) \leq \epsilon_m. \tag{59}$$

By selecting m as in (59), we typically get a higher scale leading to more accurate results at the cost of extra computational time. We therefore use (58) to compute only the VaR and we use (59) when we desire both, the VaR and the ES values (since the computation of ES implicitly involves the computation of VaR).

Once the scale of approximation m, we provide a strategy to determine the interval $[a,b]$. At the beginning of Section 3 we assume that f is well approximated at scale of resolution m in a finite interval $[a,b]\subset\mathbb{R}$, and then we defined $k_1 := \lfloor 2^m a\rfloor$ and $k_2 := \lceil 2^m b\rceil$. Thus, the determination of an appropriate truncation interval is an important issue. We use the cumulants[3] to determine an initial guess for the domain $[a,b]$.

Next we set the parameter J. Although a different J can be selected for each k, we prefer to consider a constant J, defined here by $\jmath := \lceil \log_2(\pi M_m) \rceil$ (in accordance with the error analysis performed before), where $M_m := \max_{k_1<k<k_2} M_{m,k}$. The reason is that, in practice, the computationally most involved part in (15) is the evaluation of $\hat{f}$ at the grid points. Those values can be computed only once and used by the FFT algorithm, as follows. From expression (15),

(60)

$$c^*_{m,k} = \frac{2^{m/2}}{2^{\jmath-1}} \sum_{j=1}^{2^{\jmath-1}} \Re\left[\hat{f}\left(\frac{(2j-1)\pi 2^m}{2^{\jmath}}\right) e^{\frac{ik\pi(2j-1)}{2^{\jmath}}}\right] = \frac{2^{m/2}}{2^{\jmath-1}} \Re\left[e^{\frac{ik\pi}{2^{\jmath}}} \sum_{j=0}^{2^{\jmath-1}-1} \hat{f}\left(\frac{(2j+1)\pi 2^m}{2^{\jmath}}\right) e^{\frac{2\pi ikj}{2^{\jmath}}}\right].$$

Finally, we assume that $\hat{f}\left(\frac{(2j+1)\pi 2^m}{2^{\jmath}}\right) = 0$, from $2^{\jmath-1}$ to $2^{\jmath}-1$, so that the last equality in (60) is equivalent to,

$$c^*_{m,k} = \frac{2^{m/2}}{2^{\jmath-1}} \Re\left[e^{\frac{ik\pi}{2^{\jmath}}} \sum_{j=0}^{2^{\jmath}-1} \hat{f}\left(\frac{(2j+1)\pi 2^m}{2^{\jmath}}\right) e^{\frac{2\pi ikj}{2^{\jmath}}}\right], \tag{61}$$

and therefore the FFT algorithm can be applied to compute the density coefficients $c^*_{m,k}$. The error analysis reveals that the same $\jmath$ is used to compute the risk measures in (20) and (33). As pointed out in Remark 3, this choice of $J = \jmath$ allows the acceleration of the evaluation of these risk measures by means of a discrete sine transform.

As stated in Remark 2 and shown in Section 4.1, we have that $f\left(\frac{l}{2^m}\right) \approx 2^{m/2} c_{m,l}$, for all $l \in \mathbb{Z}$ provided that the modulus of the Fourier transform $\hat{f}$ of f decays sufficiently fast. We can therefore control the quality of the truncated interval by evaluating the density f at a and b, since $f(a) \approx 2^{m/2} c_{m,k_1}$ and $f(b) \approx 2^{m/2} c_{m,k_2}$. We summarize the overall process in Algorithm 1. It is worth remarking that with all the parameters fixed beforehand, this methodology is reliable and directly applicable in practice.

1: Select the value of m such that a certain accuracy ϵ_m is reached, according to (58);
2: Determine $[a,b]$ by means of the cumulants;
3: Set $k_1 = \lfloor a/2^m \rfloor$ and $k_2 = \lceil b/2^m \rceil$;
4: Set $J = \jmath$ where $\jmath := \lceil \log_2(\pi M_m) \rceil$, $M_m := \max_{k_1<k<k_2} M_{m,k}$,
$M_{m,k} := \max\left(|2^m \mathcal{A} - k|, |2^m \mathcal{A} + k|\right)$ and $\mathcal{A} := \max(|a|,|b|)$;
5: Compute the density coefficients $c^*_{m,k}$ with the inversion formula (15) (use FFT optionally);
6: Given a tolerance ϵ_z, use a root-finding method to determine the VaR value $\mathrm{VaR}^*(\alpha)$ such that $I^*_m(J) - \alpha = 0$, where $I^*_m(J)$ is taken from (20);
7: Calculate the ES value using (33) and the VaR value computed in the former step;

Algorithm 1: Algorithm to calculate $\mathrm{VaR}^*(\alpha)$ and $\mathrm{ES}^*(\alpha)$.

5. Numerical Examples

In this section, we present a wide variety of numerical examples[4] to illustrate the accuracy, speed and robustness of SWIFT method when it is used to compute the risk measures VaR and ES within the stochastic liquidity horizon framework. We divide this section into five subsections. Section 5.1 and Section 5.2 are devoted to the delta-gamma approach, where we measure the change in value of the portfolio as a quadratic function of the change in value of the risk factors. We assume in Section 5.1 that the change in risk factors follow a Gaussian distribution and we move on to a more

[3]Given a random variable X, the cumulants are the power series coefficients of the cumulant generating function $\kappa(s) = \log \mathbb{E}(e^{sX})$.

[4]The programs have been coded in MATLAB and run under Linux OS on a laptop with Intel Core i7-5500U 2.40 GHz processor and 7.7 GB of memory.

challenging problem in Section 5.2 by assuming that these changes are driven by the heavy-tailed t distribution. In Section 5.3, Section 5.4 and Section 5.5 we consider the log-value change when the dynamics of the portfolio is driven by the Geometric Brownian motion (GBM), the Merton jump diffusion model and the Kou model respectively. The root-finding method that we pick for all the numerical examples is the bisection algorithm with the stopping criterion $\epsilon_z = 1.0e - 06$. Regarding the liquidity horizon process, we consider the type of distributions used in [6]. We select the Bernoulli distribution for the delta-gamma approach under the Gaussian model, the exponential distribution for the delta-gamma under the t distribution, the exponential distribution for the GBM, the generalised Pareto distribution for the Merton jump diffusion model and the inverse gamma distribution for the Kou model. See Table 1 and Figure 1 for a complete definition of the last three distributions and the selection of parameters in each case. We run Monte Carlo simulations as a benchmark, with one million scenarios for the risk factors and one hundred scenarios for the SLH. We consider $\epsilon_m = 1.0e{-}02$. The reason for this choice of ϵ_m is that we can expect, in the deterministic case, at most two or three digits of accuracy due to the slow convergence of MC methods. The stochastic case is less encouraging with MC simulation, since there is an additional source of randomness when considering a stochastic holding period, and these two or three digits of accuracy are not guaranteed any more.

Distribution	**Parameters**	**PDF**
Exponential	λ	$f(x) = \lambda e^{-\lambda x}$
Generalised Pareto	$k,\ \sigma,\ \theta$	$f(x) = \begin{cases} \left(\frac{1}{\sigma}\right)\left(1 + k\frac{x-\theta}{\sigma}\right)^{-1-\frac{1}{k}}, & \text{for } \theta \le x \text{ when } k > 0, \\ & \text{for } \theta \le x \le \theta - \frac{\sigma}{k} \text{ when } k < 0. \\ \frac{1}{\theta} e^{-\frac{x-\theta}{\sigma}}, & \text{for } \theta \le x \text{ when } k = 0. \end{cases}$
Inverse gamma	$\alpha,\ \beta$	$f(x) = \frac{\beta^\alpha}{\Gamma(\alpha)} x^{-\alpha-1} e^{-\frac{\beta}{x}}$

Table 1. Continuous distributions considered for the stochastic liquidity horizon.

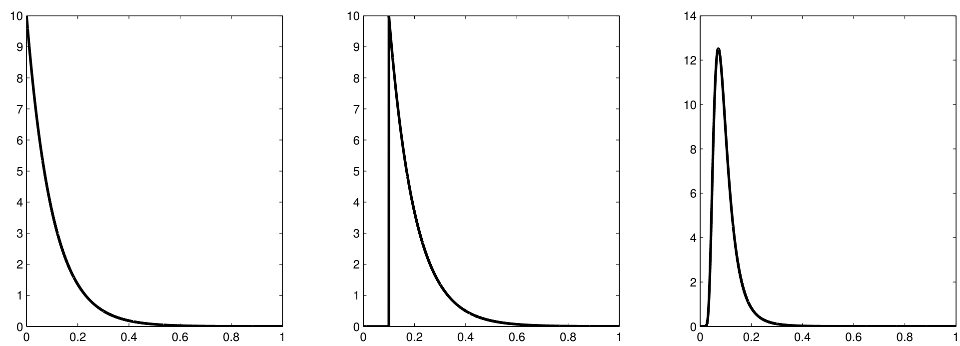

Figure 1. Exponential density with $\lambda = 10$ (left plot), generalised Pareto with $k = 0, \sigma = 0.1, \theta = 0.1$ (central plot) and inverse gamma with $\alpha = 6, \beta = 0.5$ (right plot).

5.1. **Delta-gamma approach with multivariate Gaussian model for the individual risk factors.** The delta-gamma method is a well-known approach used in market risk problems (see for instance [19]). It is based on the assumption that the change in portfolio value is a quadratic function of the changes in the risk factors, typically assumed normally distributed.

We therefore consider p risk factors $S(t) = (S_1(t), \cdots, S_p(t))^T$ at time t. We define $\Delta S = S(t + \Delta t) - S(t)$ as the change in value of the risk factors during the time interval $[t, t + \Delta t]$. Then, the change in value $\Delta V := V(t + H(t)) - V(t)$ defined in Section 1.1 is approximated by,

$$\Delta V \approx \Delta V_\gamma := \Theta \Delta t + \delta^T \Delta S + \frac{1}{2} \Delta S^T \Gamma \Delta S, \tag{62}$$

where $\Theta = \frac{\partial V}{\partial t}$, $\delta_i = \frac{\partial V}{\partial S_i}$ and $\Gamma_{i,j} = \frac{\partial^2 V}{\partial S_i \partial S_j}$ are the Greeks evaluated at time t, and the random variable $H(t)$ is the constant Δt in the deterministic case. If we assume that ΔS follows a normal distribution, then the following proposition gives us the characteristic function of ΔV_γ.

Proposition 1 (Theorem 3.2a.2 of [16]). *Assume that $\Delta S \sim \mathcal{N}(0, \Sigma)$ for some positive definite matrix Σ. Let $\lambda_1, \cdots, \lambda_p$ be the eigenvalues of $\Sigma\Gamma$, and let Λ be the diagonal matrix with these eigenvalues on the diagonal. There is a matrix C satisfying $CC^T = \Sigma$ and $C^T \Gamma C = \Lambda$. Let $d = C^T \delta$. Then, the characteristic function corresponding to $f_{\Delta V}$ is given by,*

$$\hat{f}_{\Delta V_\gamma}(u) = \mathbb{E}\left(\mathrm{e}^{-\mathrm{i}u\Delta V_\gamma}\right) = \exp\left(-\mathrm{i}u\Theta\Delta t - \frac{u^2}{2}\sum_{j=1}^{p}\frac{d_j^2}{1+\mathrm{i}\lambda_j u}\right)\prod_{j=1}^{p}(1+\mathrm{i}\lambda_j u)^{-\frac{1}{2}}, \tag{63}$$

where $u \in \mathbb{R}$.

Without loss of generality, we restrict ourselves to the univariate case $p = 1$, since the procedure to recover the density function from its characteristic function is the same. In that case the characteristic function reads,

$$\hat{f}_{\Delta V_\gamma}(u; \Delta t) = \exp\left(-iu\Theta\Delta t - \frac{d_1^2}{2}\cdot\frac{u^2}{1+i\lambda_1 u}\right)(1+i\lambda_1 u)^{-\frac{1}{2}}. \tag{64}$$

Let us first perform a consistency check for the SWIFT method by taking a base portfolio from [20] and considering three different deterministic holding periods $\Delta t = 1/365, 10/365, 30/365$. Note that we assume 365 days per year instead of trading days per year. Our portfolio is made of one short European call and half a short European put with maturity 60 days. The underlying asset at time t is 100 with volatility level $\sigma = 0.3$, interest rate 0.1 and strike price 101 for each option. Following similar steps than in [20] we select,

$$\Sigma = \left(S(t)\sigma\sqrt{\Delta t}\right)^2, \quad \Gamma = \sum_{i=1}^{n} x_i \frac{\partial^2 v_i}{\partial S^2}, \quad C = S(t)\sigma\sqrt{\Delta t}, \quad \delta = \sum_{i=1}^{n} x_i \frac{\partial v_i}{\partial S},$$

where n represents the number of assets in the portfolio, x_i is the amount of asset i and v_i the value of asset i. Finally,

$$[a, b] = [\kappa_1 - L\sqrt{\kappa_2}, \kappa_1 + L\sqrt{\kappa_2}], \tag{65}$$

where κ_1 and κ_2 stand for the first and second cumulants[5] respectively,

$$\begin{aligned} \kappa_1 &= \frac{1}{2}\mathrm{tr}\,(\Gamma\Sigma) + \Theta\Delta t, \\ \kappa_2 &= \frac{1}{2}\mathrm{tr}\left((\Gamma\Sigma)^2\right) + \delta^T\Sigma\delta. \end{aligned} \tag{66}$$

The Greeks are computed using the Black-Scholes formula and $L = 10$ in all the numerical examples hereinafter. As stated in Section 4.1, the coefficients $|c_{m,k}|$ can be well approximated by $\frac{1}{2^{m/2}} f\left(\frac{k}{2^m}\right)$. We can therefore assess the suitability of the selected interval $[a, b]$ by evaluating the value of the density at the extremes of the interval, this is, $f\left(\frac{k_1}{2^m}\right) \approx 2^{m/2} c_{m,k_1}$ and $f\left(\frac{k_2}{2^m}\right) \approx 2^{m/2} c_{m,k_2}$ since these two coefficients have been already calculated. As pointed out in [20], when $p = 1$ we know the shape of the density and the number of modes (Corollary 1 of [20]). Further, from Corollary 1 and Corollary 2 of [20], we know that if $\Gamma_{1,1} > 0$ then the density function is supported on $[\mathcal{B}, +\infty)$, with $\mathcal{B} := -\frac{d_1^2}{2\lambda_1} + \Theta\Delta t$, while when $\Gamma_{1,1} < 0$ then the density function is supported on $(-\infty, \mathcal{B}]$. Thus, we select the interval $[\mathcal{B}, \kappa_1 + L\sqrt{\kappa_2}]$ in the first case and $[\kappa_1 - L\sqrt{\kappa_2}, \mathcal{B}]$ in the second case.

We present the results of our numerical experiments in Table 2. The benchmark solution is calculated by means of Partial Monte Carlo (PMC) simulation, which basically means that we simulate ΔS and use the approximation in (62). For sake of completeness we give the results corresponding to Full Monte Carlo (FMC) where we revaluate the portfolio with Black-Scholes formula for each

[5] Look at Theorem 3.3.2 of [16] for details.

new value of the underlying risk factor. We show the scale of approximation calculated with the error formula (58). We observe that the absolute error reported is in accordance with ϵ_m. It is worth remarking that for the cases $\Delta t = 10/365$ and $\Delta t = 30/365$ the VaR computation is somewhat more challenging than in the case $\Delta t = 1/365$, due to the asymptotic behaviour of the densities at $\mathcal{B}$ (see Figure 2 and the details provided in Section 4.4 and Section 5 of [20]). In these two extreme cases the bisection method does not work properly, since the condition $g(a) \cdot g(b) < 0$ with $g(l_\alpha) = I^*_m(J) - \alpha$ is not satisfied. When this situation occurs, we set $\mathrm{VaR}^*(\alpha) = \mathcal{B}$.

Δt	PMC	FMC	SWIFT	Absolute error	m
1/365	0.9024	0.8792	0.9038	$1.4e-03$	2
10/365	1.7044	1.5430	1.7050	$5.3e-04$	6
30/365	3.0434	2.8148	3.0439	$5.0e-04$	6

Table 2. Absolute errors with respect to Partial Monte Carlo simulation, corresponding to the computation of VaR with deterministic holding period Δt and $\alpha = 0.99$.

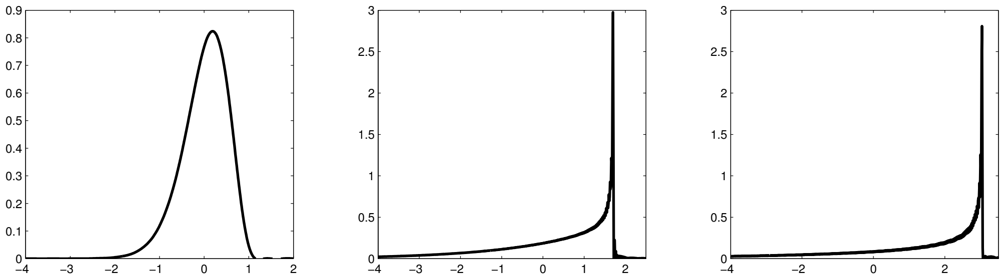

Figure 2. Density plots for $\Delta t = 1/365$ (left), $\Delta t = 10/365$ (central) and $\Delta t = 30/365$ (right).

Next, we study the performance of SWIFT method within the SLH framework. We assume that $H(t)$ follows the Bernoulli distribution and we distinguish the three different cases represented in Table 3, where $H(t)$ takes the value $h_1 = 10/365$ with probability p and $h_2 = 30/365$ with probability $1-p$. The only different issue within the SLH framework with respect to the deterministic case is the need of computing the appropriate characteristic function to be used by SWIFT method. Since we know the characteristic function in the deterministic case, we apply the law of iterated expectations,

$$\hat{f}_{\Delta V_\gamma}(u) = \mathbb{E}[e^{-iu\Delta V_\gamma}] = \mathbb{E}[\mathbb{E}[e^{-iu\Delta V_\gamma}|H(t)]] = p\hat{f}_{\Delta V_\gamma}(u;h_1) + (1-p)\hat{f}_{\Delta V_\gamma}(u;h_2). \quad (67)$$

The interval of approximation in this case is calculated as,

$$[a,b] = [\min\{a_{h_1}, a_{h_2}\}, \max\{b_{h_1}, b_{h_2}\}],$$

where $[a_{h_1}, b_{h_1}]$ and $[a_{h_2}, b_{h_2}]$ correspond to the intervals calculated in the deterministic case with $h_1 = 10/365$ and $h_2 = 30/365$ respectively. We observe that again, the absolute error is in accordance with ϵ_m and the scale calculated with formula (58) is $m = 5$ in all three cases.

$H(t)$	PMC	SWIFT	Absolute error	m
$\mathbb{P}(h_1) = 0.25, \mathbb{P}(h_2) = 0.75$	3.0430	3.0439	$8.3e-04$	5
$\mathbb{P}(h_1) = 0.5, \mathbb{P}(h_2) = 0.5$	3.0415	3.0425	$1.0e-03$	5
$\mathbb{P}(h_1) = 0.75, \mathbb{P}(h_2) = 0.25$	3.0312	3.0327	$1.5e-03$	5

Table 3. Absolute errors with respect to Partial Monte Carlo simulation, corresponding to the computation of VaR with stochastic holding period driven by a Bernoulli distribution and $\alpha = 0.99$.

5.2. **Delta-gamma approach with multivariate t distribution for the individual risk factors.** Next, we consider the delta-gamma approach presented in [13] where the underlying risk factors are heavy-tailed distributed by means of the t distribution. We build upon the work exposed in [13] for the deterministic case and we extend that approach to the stochastic liquidity horizon framework. A t distribution is characterized by the number of degrees of freedom ν. The tails of its density decay at a polynomial rate of $x^{-\nu}$, so the parameter ν determines the heaviness of the tail and the number of finite moments. Let t_ν be the univariate t distribution with ν degrees of freedom, which has density,

$$f_{t_\nu}(x) = \frac{\Gamma\left(\frac{1}{2}(\nu+1)\right)}{\sqrt{\nu\pi}\,\Gamma\left(\frac{1}{2}\nu\right)}\left(1+\frac{x^2}{\nu}\right)^{-(\nu+1)/2}, \quad -\infty < x < \infty, \tag{68}$$

where $\Gamma(\cdot)$ denotes the gamma function. The multivariate t distribution has density,

$$f_{\nu,\Sigma}(x) = \frac{\Gamma\left(\frac{1}{2}(p+\nu)\right)}{(\nu\pi)^{p/2}\Gamma\left(\frac{1}{2}\nu\right)|\Sigma|^{1/2}}\left(1+\frac{1}{\nu}x^T\Sigma^{-1}x\right)^{-\frac{1}{2}(p+\nu)}, \quad x \in \mathbb{R}^p, \tag{69}$$

where Σ is a symmetric, positive definite matrix. If $\nu > 2$, then $\nu\Sigma/(\nu-2)$ is the covariance matrix of $f_{\nu,\Sigma}$. The multivariate $t_{\nu,\Sigma}$ density (69) belongs to the class of scale mixtures of normals. Thus, it has representation as the distribution of the product of a multivariate normal random vector and a univariate random variable independent of the normal. If $(X_1,\cdots,X_p)$ has density $f_{\nu,\Sigma}$, then,

$$(X_1,\cdots,X_p) \sim \frac{(\xi_1,\cdots,\xi_p)}{\sqrt{Y/\nu}}, \tag{70}$$

where $\xi = (\xi_1,\cdots,\xi_p) \sim \mathcal{N}(0,\Sigma)$, $Y \sim \chi^2_\nu$ (chi-square with ν degrees of freedom), and ξ and Y are independent.

If we assume within this section that ΔS in (62) follows the multivariate t distribution in (69), then $\Delta S \sim \dfrac{\xi}{\sqrt{Y/\nu}}$, thanks to the ratio representation (70), and ΔS is therefore modelled as a scale mixture of normals. For sake of simplicity in the exposition, we give a brief summary of the methodology developed in [13], where the authors define the loss $L = -\Delta V$ and,

$$L \approx a_0 + a^T\Delta S + \Delta S^T A \Delta S \equiv a_0 + \mathcal{Q}, \tag{71}$$

with $a_0 = -\Theta\Delta t$, $a = -\delta$ and $A = -\frac{1}{2}\Gamma$.

By defining,

$$\mathcal{Q}_x := \left(\frac{Y}{\nu}\right)(\mathcal{Q}-x), \tag{72}$$

and observing that $\mathbb{P}(\mathcal{Q} \le x) = \mathbb{P}(\mathcal{Q}_x \le 0) \equiv F_x(0)$, we can compute $\mathbb{P}(\mathcal{Q} \le x)$ by finding the characteristic function of $\mathcal{Q}_x$ and then we invert it to find $\mathbb{P}(\mathcal{Q}_x \le 0)$. The following theorem gives us the characteristic function of $\mathcal{Q}_x$.

Theorem 3 (Theorem 3.1 of [13])**.** *Let $\lambda_1 \ge \lambda_2 \ge \cdots \ge \lambda_p$ be the eigenvalues of ΣA and let Λ be the diagonal matrix with these eigenvalues on the diagonal. There is a matrix C satisfying $CC^T = \Sigma$ and $C^TAC = \Lambda$. Let $b = a^TC$. Then $\mathbb{P}(\mathcal{Q} \le x) = F_x(0)$, where the distribution F_x has moment generating function,*

$$\phi_x(\theta) = \left(1+\frac{2\theta x}{\nu}-\sum_{j=1}^{p}\frac{\theta^2 b^2/\nu}{1-2\theta\lambda_j}\right)^{-\nu/2}\prod_{j=1}^{p}\frac{1}{\sqrt{1-2\theta\lambda_j}}. \tag{73}$$

The characteristic function of $\mathcal{Q}_x$ is given by $\hat{f}_{\mathcal{Q}_x} = \mathbb{E}[\exp(-i\omega\mathcal{Q}_x)] = \phi_x(-i\omega)$.

We can easily obtain a closed-form expression for the Fourier transform $\hat{F}_{\mathcal{Q}_x}$ of $F_{\mathcal{Q}_x}$ from $\hat{f}_{\mathcal{Q}_x}$ integrating by parts. If we use the SWIFT method to recover $F_{\mathcal{Q}_x}$ from $\hat{F}_{\mathcal{Q}_x}$, and we have into account that,

$$F_{\Delta V}(y) = 1 - F_L(-y) = 1 - F_{\mathcal{Q}}(-y-a_0) = 1 - F_{\mathcal{Q}_{(-y-a_0)}}(0), \tag{74}$$

then we can compute the VaR value by applying a bisection method to to find l such that,

$$1 - \alpha - F_{\mathcal{Q}_{-(l+a_0)}}(0) = 0. \tag{75}$$

Whilst in Section 5.1 only one Fourier inversion was performed, it is worth remarking that, in this case, each step in the bisection method involves a Fourier inversion by means of SWIFT method. This is clearly a challenge in terms of computation and we can tackle this problem only with a very efficient numerical method to avoid the propagation of the error.

As in Section 5.1 and without loss of generality, we restrict ourselves to the univariate case $p = 1$. We use first a deterministic holding period $\Delta t = 1/365$. Our portfolio is the same as in Section 5.1, made of one short European call and half a short European put with maturity 60 days. The underlying asset at time t is 100 with volatility level $\sigma = 0.3$, interest rate 0.1 and strike price 101 for each option. Note that the scale parameter m is recalculated at each bisection step following the tolerance error $\epsilon_m = 1.0e-02$ set at the beginning of Section 5. We present the results of the numerical experiments in Table 4 for values of $\nu \in \{3, 5, 7\}$. The benchmark solution is calculated by means of PMC with one million scenarios as mentioned at the beginning of Section 5. To show the accuracy of the proposed numerical method, we have added some extra numerical experiments in Table 5 with ten million scenarios for PMC to be used as a benchmark for SWIFT method with $\epsilon_m = 1.0e-03$ and $\epsilon_m = 1.0e-04$ respectively.

ν	PMC (10^6)	SWIFT	Absolute error ($\epsilon_m = 10^{-2}$)
3	0.9438	1.0201	$7.6e-02$
5	0.9562	1.0119	$5.6e-02$
7	0.9456	0.9678	$2.2e-02$

Table 4. Absolute errors with respect to Partial Monte Carlo simulation, corresponding to the computation of VaR with deterministic holding period $\Delta t = 1/365, \alpha = 0.99$ and $\nu = 3, 5, 7$.

ν	PMC (10^7)	Absolute error ($\epsilon_m = 10^{-3}$)	Absolute error ($\epsilon_m = 10^{-4}$)
3	0.9438	$5.2e-03$	$2.7e-04$
5	0.9548	$2.9e-03$	$1.6e-04$
7	0.9447	$3.8e-03$	$2.6e-04$

Table 5. Absolute errors with respect to Partial Monte Carlo simulation, corresponding to the computation of VaR with deterministic holding period $\Delta t = 1/365, \alpha = 0.99$ and $\nu = 3, 5, 7$.

Next we study the performance of SWIFT method within the SLH framework. We consider the same portfolio as in the deterministic case and we assume that $H(t)$ follows an exponential distribution with parameter $\lambda = 10$. Since the holding period is not deterministic, we cannot apply directly the bisection method in (75). To circumvent this problem, we condition on a realization of H and use the law of iterated expectations,

(76)

$$\begin{aligned} F_{\mathcal{Q}_{-(l+\Theta H(t))}}(0) &= \mathbb{P}(\mathcal{Q}_{-l-\Theta H(t)} \le 0) = \mathbb{E}\left[\mathbb{1}_{\{\mathcal{Q}_{-(l+\Theta H(t))} \le 0\}}\right] = \mathbb{E}\left[\mathbb{E}\left[\mathbb{1}_{\{\mathcal{Q}_{-(l+\Theta H(t))} \le 0\}} | H(t) = h\right]\right] \\ &= \int_{\mathbb{R}} \mathbb{E}\left[\mathbb{1}_{\{\mathcal{Q}_{-(l+\Theta h)} \le 0\}}\right] f_H(h) dh = \int_{\mathbb{R}} F_{\mathcal{Q}_{-(l+\Theta h)}}(0) f_H(h) dh, \end{aligned}$$

where $f_H(h) = 10 \exp(-10h)$ is the probability density function of the stochastic holding period. Now we can apply the bisection method to find l such that,

$$1 - \alpha - F_{\mathcal{Q}_{-(l+\Theta H(t))}}(0) = 0. \tag{77}$$

The integral in the right-hand side of (76) must be calculated at each iteration of the bisection method. The integral is evaluated by means of the trapezoidal rule and the infinite integration domain is replaced by the finite domain $[0, h^*]$, where h^* is such that $F_H(h^*) < 1.e-06$, being F_H the CDF of $H(t)$. Note that for each quadrature point h, we calculate $F_{\mathcal{Q}_{-(l+\Theta h)}}(0)$ as in the deterministic case. The results are shown in Table 6. We run one hundred times the PMC method and we consider the average as the benchmark solution, giving also a 95% confidence interval. It is worth remarking that Monte Carlo simulation is extremely demanding in terms of computing due to the heavy-tailed distribution combined with the stochastic holding period.

ν	PMC	95% CI	SWIFT	Absolute error
3	10.1776	$[8.0220, 13.5035]$	10.0803	$9.7e-02$
5	9.8275	$[7.4039, 13.2777]$	9.5490	$2.8e-01$
7	9.7135	$[7.6791, 12.5971]$	9.5047	$2.1e-01$

Table 6. Absolute errors with respect to Partial Monte Carlo simulation, corresponding to the computation of VaR with stochastic holding period driven by an exponential distribution with $\lambda = 10$ and $\alpha = 0.99$.

5.3. **Geometric Brownian Motion.** In this section we consider that our portfolio V_t follows GBM dynamics,

$$dV_t = \mu V_t\,dt + \sigma V_t\,dW_t, \tag{78}$$

where, as usual, μ represents the drift and σ the volatility. As it was stated in Section 1.1, we are interested in measuring the change in the log-value of the portfolio rather than in the value itself. Thus, we consider $X = \ln(V(t+H(t))) - \ln(V(t))$, where $H(t)$ is the constant value Δt in the deterministic case. It is well known that X follows a normal distribution with mean $\left(\mu - \frac{\sigma^2}{2}\right)\Delta t$ and variance $\sigma^2 \Delta t$, its characteristic function reads,

$$\hat{f}_X(u;\Delta t) = \exp\left(-i\left(\mu - \frac{\sigma^2}{2}\right)\Delta t u - \frac{\sigma^2 \Delta t}{2}u^2\right). \tag{79}$$

The first two cumulants are $\kappa_1 = \left(\mu - \frac{\sigma^2}{2}\right)\Delta t$ and $\kappa_2 = \sigma^2\Delta t$, and we determine the interval of approximation $[a, b]$ following the rule-of-thumb (65). In this particular case there are closed form solutions for VaR and ES values,

$$\mathrm{VaR}(\alpha) = \left(\mu - \frac{\sigma^2}{2}\right)\Delta t + \sigma\sqrt{\Delta t}\Phi^{-1}(\alpha), \quad \mathrm{ES}(\alpha) = \left(\mu - \frac{\sigma^2}{2}\right)\Delta t + \frac{\sigma\sqrt{\Delta t}\phi(\Phi^{-1}(\alpha))}{1-\alpha}, \tag{80}$$

where ϕ stands for the PDF of a normal standard and Φ is its CDF, and we use them as the benchmark solution. We present the numerical experiments in Table 7. We consider three different confidence levels α, where $\alpha = 0.99$ is the traditional regulatory confidence level to measure the VaR while $\alpha = 0.975$ has become the new regulatory confidence level to measure the ES. Since we aim at computing both risk measures, we use the error formula (59) to estimate the parameter m. We see again that the ES error is in accordance with the fixed tolerance ϵ_m. We observe that the VaR error is extremely small due to the the fact that formula (59) is equivalent to use formula (58) with a tolerance error of $(1-\alpha)\epsilon_m$. To show the power of approximation of SWIFT method, we note that when $\epsilon_m = 1.e-05$ and $\alpha = 0.99$ then $m = 7$ and the ES error is $5.1e-06$.

		VaR			ES		
α	m	Exact	SWIFT	Absolute Error	Exact	SWIFT	Absolute error
0.95	6	0.0430	0.0430	$1.5e-07$	0.0539	0.0594	$5.4e-03$
0.975	6	0.5012	0.0512	$2.8e-07$	0.0611	0.0720	$1.1e-02$
0.99	6	0.0608	0.0608	$1.9e-07$	0.0697	0.0969	$2.7e-02$

Table 7. Absolute errors for VaR and ES values with respect to the exact formula (80) when V_t follows a GBM dynamics with $\mu = 0.1, \sigma = 0.5$ and $\Delta t = 1/365$.

Next, we consider the GBM dynamics in combination with an exponential random variable to drive the SHL. In this case,

$$\hat{f}_X(u) = \mathbb{E}[e^{-iuX}] = \mathbb{E}[\mathbb{E}[e^{-iuX} \mid H(t)]] = \mathbb{E}[\hat{f}_X(u;h)] = \int_{\mathbb{R}^+} \hat{f}_X(u;h) f_H(h)dh, \tag{81}$$

where $f_H(h) = \lambda \exp(-\lambda h)$. The integral in (81) can be solved analytically yielding,

$$\hat{f}_X(u) = \frac{-\lambda}{\lambda + i\left(\mu - \frac{\sigma^2}{2}\right)u + \frac{1}{2}\sigma^2 u^2}. \tag{82}$$

We use the expression (82) to calculate the scale of approximation m. We can also use the same expression to compute the cumulants. However, if we observe the cumulants in the deterministic case, we realize that they are increasing functions of Δt. We therefore consider the union of the two intervals corresponding to the minimum ($h_1 = 0$) and maximum holding period, where the maximum is determined by h_2 such that $F_H(h_2) < 1.e-06$, and F_H stands for the CDF of $H(t)$,

$$[a, b] = [\min\{a_{h_1}, a_{h_2}\}, \max\{b_{h_1}, b_{h_2}\}], \tag{83}$$

where $a_{h_1} = b_{h_1} = 0$, $a_{h_2} = \left(\mu - \frac{\sigma^2}{2}\right)h_2 - L\sigma\sqrt{h_2}$ and $b_{h_2} = \left(\mu - \frac{\sigma^2}{2}\right)h_2 + L\sigma\sqrt{h_2}$. We consider two benchmark solutions in this case. First of all, we run MC simulations like in Section 5.1 with the initial value of the portfolio $V_0 = 100$. The results are presented in Table 8, where in general the absolute error is of order $1.e-02$.

		VaR			ES		
α	m	MC	SWIFT	Absolute Error	MC	SWIFT	Absolute error
0.95	7	0.2331	0.2533	$2.0e-02$	0.3378	0.3638	$2.6e-02$
0.975	7	0.3064	0.3300	$2.4e-02$	0.4103	0.4404	$3.0e-02$
0.99	8	0.4005	0.4313	$3.1e-02$	0.5049	0.5418	$3.7e-02$

Table 8. Absolute errors for VaR and ES values with respect to MC simulation when V_t follows a GBM dynamics with $\mu = 0.1, \sigma = 0.5$. The SLH is driven by an exponential distribution with $\lambda = 10$.

However, in order to really assess the accuracy of SWIFT method, we use a second benchmark solution. We consider the numerical formulae employed in [6] for VaR value,

$$\int_0^\infty \Phi\left(\frac{\mathrm{VaR}(\alpha) - \left(\mu - \frac{\sigma^2}{2}\right)h}{\sigma\sqrt{h}}\right) f_H(h)dh = \alpha, \tag{84}$$

and ES value,

$$\mathrm{ES}(\alpha) = \frac{1}{1-\alpha}\int_0^\infty \left(\left(\mu - \frac{\sigma^2}{2}\right)h\Phi\left(\frac{\left(\mu - \frac{\sigma^2}{2}\right)h - \mathrm{VaR}(\alpha)}{\sigma\sqrt{h}}\right) + \sigma\sqrt{h}\phi\left(\frac{\mathrm{VaR}(\alpha) - \left(\mu - \frac{\sigma^2}{2}\right)h}{\sigma\sqrt{h}}\right)\right) f_H(h)dh. \tag{85}$$

We use the MATLAB function `integral` to numerically solve the integrals in (84) and (85), and the MATLAB function `fzero` as a root-finding method in (84). The results are presented in Table 9, where we can observe very accurate results for VaR as well as for ES values.

5.4. **Merton jump-diffusion model.** As pointed out in [9], jump-diffusion models assume that the evolution of prices is given by a diffusion process, punctuated by jumps at random intervals. Here the jumps represent rare events like crashes and large drawdowns. Such an evolution can be represented by modelling the log-price as a Lévy process with a nonzero Gaussian component and a jump part, which is a compound Poisson process with finitely many jumps in every time interval. Examples of such models are the MJD model with Gaussian jumps [18] and the Kou model with double exponential jumps [14]. In this section we consider the MJD model for driving the dynamics of the value of the portfolio V_t, whilst next section is devoted to the Kou model.

		VaR			ES		
α	m	Reference	SWIFT	Absolute Error	Reference	SWIFT	Absolute error
0.95	7	0.2533	0.2533	$1.2e-06$	0.3639	0.3638	$6.2e-05$
0.975	7	0.3300	0.3300	$3.2e-06$	0.4405	0.4404	$1.3e-04$
0.99	8	0.4313	0.4313	$8.5e-06$	0.5418	0.5418	$5.5e-05$

Table 9. Absolute errors for VaR and ES values with respect to the formulae (84) and (85) when V_t follows a GBM dynamics with $\mu = 0.1, \sigma = 0.5$. The SLH is driven by an exponential distribution with $\lambda = 10$.

The process V_t is assumed to follow the stochastic differential equation,

$$dV_t = (\mu - \lambda\kappa)V_t dt + \sigma V_t dW_t + (e^J - 1)V_t dq_t, \tag{86}$$

where q_t represents a Poisson process with mean arrival rate λ, J has normally distributed jumps with mean μ_J and standard deviation σ_J, $\kappa = \mathbb{E}[e^J - 1]$ and W_t is a standard Brownian motion process. The characteristic function of $X = \ln(V(t + H(t))) - \ln(V(t))$ in the deterministic case when $H(t)$ is Δt reads,

$$\hat{f}_X(u;\Delta t) = \exp\left(-i\left(\mu - \lambda\kappa - \frac{\sigma^2}{2}\right)\Delta t u - \frac{\sigma^2\Delta t}{2}u^2 + \lambda\Delta t\left(e^{-i\mu_J u - \frac{\sigma_J^2 u^2}{2}} - 1\right)\right), \tag{87}$$

and we use the cumulants,

$$\begin{aligned} \kappa_1 &= \mu_J\lambda\Delta t + \left(\mu - \lambda\kappa - \frac{\sigma^2}{2}\right)\Delta t, \\ \kappa_2 &= \left(\sigma^2 + \lambda\left(\mu_J^2 + \sigma_J^2\right)\right)\Delta t, \\ \kappa_4 &= \left(\mu_J^4 + 6\sigma_J^2\mu_J^2 + 3\sigma_J^4\right)\lambda\Delta t. \end{aligned} \tag{88}$$

To be more precise, the initial guess that we use for the MJD and Kou models to determine the truncation interval is,

$$[a,b] = \left[\kappa_1 - L\sqrt{\kappa_2 + \sqrt{\kappa_4}}, \kappa_1 + L\sqrt{\kappa_2 + \sqrt{\kappa_4}}\right]. \tag{89}$$

The benchmark solution is MC with $V_0 = 100$, since there are not closed form solutions in this case to compute the risk measures. We present the results in Table 10, where we illustrate both, the deterministic case with $\Delta t = 5/365$, and the stochastic case with the SLH driven by a generalised Pareto distribution. We chose the regulatory level $\alpha = 0.975$. The characteristic function within the stochastic case is obtained numerically solving the integral in (81) by means of the trapezoidal rule. The truncation of the integration domain and the determination of the interval $[a,b]$ follows an entirely analogous process as in Section 5.3. We observe that SWIFT method performs well working at a low scale $m = 3$ in the challenging stochastic case. We measure the CPU time in seconds of the overall process, including the VaR as well as the ES computation. This measurement reveals the efficiency of the methodology capable to accurately estimate the risk measures in less than 0.1 second. We note that the stochastic case is more involved, since in this case, the characteristic function is obtained numerically.

		VaR			ES			
$H(t)$	m	MC	SWIFT	Absolute Error	MC	SWIFT	Absolute error	CPU time (sec.)
$5/365$	5	0.1171	0.1172	$8.2e-05$	0.1601	0.1555	$4.6e-03$	0.02
SLH	3	0.4726	0.4730	$3.7e-04$	0.6081	0.5557	$5.2e-02$	0.08

Table 10. Absolute errors for VaR and ES values with respect to MC simulation when V_t follows a MJD dynamics with $\mu = 0.1, \sigma = 0.5, \lambda = 0.6, \mu_J = 0.1, \sigma_J = 0.2$. In the deterministic case $\Delta t = 5/365$. The SLH is driven by a generalised Pareto distribution with $k = 0, \sigma = 0.1, \theta = 0.1$. The confidence level is $\alpha = 0.975$.

5.5. **Kou model.** Finally, we consider that the portfolio V_t follows the dynamics of the Kou model. This model is also called the double exponential jump-diffusion model and it can reproduce the leptokurtic feature of the return distribution, which has semi-heavy (exponential) tails. Given a process V_t, it is modelled as,

$$dV_t = (\mu - \lambda\kappa)V_t dt + \sigma V_t dW_t + \left(e^J - 1\right) dq_t, \tag{90}$$

where q_t is a Poisson process with mean arrival rate λ and J has double exponentially distributed jumps with density,

$$f_J(y) = p\eta_1 \mathrm{e}^{-\eta_1 y}\mathbb{1}_{y\geq 0} + q\eta_2 \mathrm{e}^{\eta_2 y}\mathbb{1}_{y<0}, \tag{91}$$

with $\eta_1 > 1$, $\eta_2 > 0$ governing the decay of the tails and $p, q \geq 0, p + q = 1$, with p representing the probability of an upward jump, and $\kappa = \mathbb{E}[e^J - 1]$. The characteristic function of $X = \ln(V(t + H(t))) - \ln(V(t))$ in the deterministic case when $H(t)$ is Δt reads,

$$\hat{f}_X(u) = \exp\left(-i\left(\mu - \lambda\kappa - \frac{\sigma^2}{2}\right)\Delta t u - \frac{\sigma^2\Delta t}{2}u^2 - \mathrm{i}\lambda\left(\frac{p}{\eta_1 + \mathrm{i}u} + \frac{q}{\eta_2 - \mathrm{i}u}\right)\Delta t u\right), \tag{92}$$

and the cumulants are,

$$\begin{aligned}
\kappa_1 &= \left(\mu - \lambda\kappa - \frac{\sigma^2}{2}\right)\Delta t + \left(\frac{p}{\eta_1} + \frac{q}{\eta_2}\right)\lambda\Delta t, \\
\kappa_2 &= \left(\frac{p}{\eta_1^2} - \frac{q}{\eta_2^2}\right)\lambda\Delta t + \sigma^2\Delta t, \\
\kappa_4 &= \left(\frac{p}{\eta_1^4} - \frac{q}{\eta_2^4}\right)\lambda\Delta t.
\end{aligned} \tag{93}$$

In Table 11 we present the VaR and ES values computed at the regulatory level $\alpha = 0.975$. In the deterministic case we consider $\Delta t = 5/365$ and the inverse gamma distribution is used for governing the SLH dynamics. The benchmark solution is MC and $V_0 = 100$. We observe that the absolute errors are in line with those obtained in the former sections when comparing with MC.

		VaR			ES		
$H(t)$	m	MC	SWIFT	Absolute Error	MC	SWIFT	Absolute error
$5/365$	5	0.1109	0.1110	$1.3e-04$	0.2225	0.1670	$5.6e-02$
SLH	4	0.3262	0.3335	$7.4e-03$	0.8129	0.8058	$7.1e-03$

Table 11. Absolute errors for VaR and ES values with respect to MC simulation when V_t follows a Kou dynamics with $\mu = 0.1, \sigma = 0.5, \lambda = 0.6, \eta_1 = 1.5, \eta_2 = 1.8, p = 0.5$. In the deterministic case $\Delta t = 5/365$. The SLH is driven by an inverse gamma distribution with $\alpha = 6, \beta = 0.5$. The confidence level is $\alpha = 0.975$.

6. Conclusions

In this work we present a numerical method to efficiently calculate VaR and ES values within a stochastic liquidity horizon framework. We therefore focus on two aspects underlined as key regulatory changes by the Basel Committee of Banking Supervision, like moving from VaR to ES and considering the incorporation of the risk of market illiquidity. The estimation of the risk measures with a stochastic holding period appears to be particularly challenging in terms of computational power.

For the aforementioned reasons, we employ the SWIFT method, which recovers the density function of the change in value of a certain portfolio from its characteristic function. The density function is approximated by a finite expansion in terms of Shannon wavelets and the coefficients of the approximation are readily obtained by a Fourier transform inversion. This method relies on the availability of the characteristic function, which is known in closed form for many interesting processes in finance. We consider the well-known delta-gamma approach for modelling the change in value of the portfolio under normal and t-distributed risk factors, as well as the GBM, MJD and Kou models for the log-value change of the portfolio, where these two last models incorporate a jump component in the dynamics. As for the dynamics of the SLH, we consider the Bernoulli distribution, the exponential, the generalised Pareto and the inverse gamma in combination with the delta-gamma approach, and the GBM, MJD and Kou dynamics. We carry out a detailed error analysis and we provide a prescription on how to select the parameters of the numerical method, making this technique more robust, reliable and applicable in practice. We leave for future work the calibration of the parameters of the models employed, as well as the SLH, with real market data. Another interesting extension of the present work would be the consideration of different risk factors having different liquidity horizons in line with the regulatory rules of the Basel Committee on Banking Supervision. The modelling of dependence between the stochastic holding period and log-returns of assets is a topic of interest in practice for future developments.

Acknowledgment

The research leading to these results has received funding from La Caixa Foundation. G. C.-P. acknowledges AGAUR-Generalitat de Catalunya for funding under its doctoral scholarship programme. G. C.-P. and L. O.-G. acknowledge the Spanish Ministry of Economy and Competitiveness (MINECO) for funding under grant MTM2013-40782-P.

References

[1] P. Artzner, F. Delbaen, J. M. Eber, and D. Heath. Coherent measures of risk. *Mathematical Finance*, 9(3):203–228, 1999.
[2] Basel Committee on Banking Supervision. Messages from the academic literature on risk measurement for the trading book. *Bank for International Settlements*, 2011.
[3] Basel Committee on Banking Supervision. Fundamental review of the trading book. *Bank for International Settlements*, 2012.
[4] Basel Committee on Banking Supervision. Fundamental review of the trading book: a revised market risk framework. *Bank for International Settlements*, 2013.
[5] Basel Committee on Banking Supervision. Minimum capital requirements for market risk. *Bank for International Settlements*, 2016.
[6] D. Brigo and C. Nodio. A random holding period approach for liquidity-inclusive risk management. In K. Glau, editor, *Innovations in Quantitative Risk Management*, volume 99. Springer Proceeding in Mathematics & statistics 99, 2015.
[7] C. Cattani. Shannon wavelets theory. *Mathematical problems in Enigneering*, 2008:164808, 2008.
[8] G. Colldeforns-Papiol, L. Ortiz-Gracia, and C. W. Oosterlee. Multidimensional Shannon wavelet inverse Fourier technique for pricing financial european options. *Submitted for publication*, 2016.
[9] R. Cont and P. Tankov. *Financial modelling with Jump processes*. Chapman & Hall / CRC Press, 2004.
[10] D.M. Dang and L. Ortiz-Gracia. A dimension reduction Shannon-wavelet based method for option pricing. *Submitted for publication*, 2015.
[11] I. Daubechies. *Ten Lectures on Wavelets*. Society for Industrial and Applied Mathematics, 1992.
[12] W. B. Gearhart and H. S. Shultz. The function sin(x)/x. *The College Mathematics Journal*, 21(2):90–99, 1990.
[13] P. Glasserman, P. Heidelberger, and P. Shahabuddin. Portfolio value-at-risk with heavy-tailed risk factors. *Mathematical Finance*, 12(3):239–269, 2002.
[14] S. G. Kou. A jump-diffusion model for option pricing. *Management Science*, 48(8):1086–1101, 2002.
[15] S. C. Maree, L. Ortiz-Gracia, and C. W. Oosterlee. Pricing early-exercise and discrete barrier options by Shannon wavelet expansions. *Submitted for publication*, 2015.
[16] A. M. Mathai and Serge B. Provost. *Quadratic forms in random variables*, volume 126 of *Statistics: Textbooks and Monographs*. Marcel Dekker, Inc., New York, 1992. Theory and applications.
[17] A. J. McNeil, R. Frey, and P. Embrechts. *Quantitative risk management: concepts, techniques and tools*. Princeton University Press, 2015.
[18] R. C. Merton. Option pricing when underlying stock returns are discontinuous. *Journal of Financial Economics*, 3:125–144, 1976.
[19] J. Mina and A. Ulmer. Delta-gamma four ways. *RiskMetrics Group*, LLC, 1999.
[20] L. Ortiz-Gracia and C. W. Oosterlee. Efficient VaR and Expected Shortfall computations for nonlinear portfolios within the delta-gamma approach. *Applied Mathematics and Computation*, 244:16–31, 2014.
[21] L. Ortiz-Gracia and C. W. Oosterlee. A highly efficient Shannon wavelet inverse Fourier technique for pricing European options. *SIAM Journal on Scientific Computing*, 38(1):B18–B143, 2016.
[22] B. M. Quine and S. M. Abrarov. Application of the spectrally integrated voigt function to line-by-line radiative transfer modelling. *Journal of Quantitative Spectroscopy & radiative Transfer*, 244:37–48, 2013.

[23] F. Stenger. *Handbook of Sinc numerical methods*. Chapman & Hall/CRC Numerical Analysis and Scientific Computing. CRC Press, Boca Raton, FL, 2011.

Gemma Colldeforns-Papiol
Centre de Recerca Matemàtica
Campus de Bellaterra, Edifici C
08193 Bellaterra (Barcelona)
Spain
and
Departament de Matemàtiques
Universitat Autònoma de Barcelona
08193 Bellaterra (Barcelona)
Spain
E-mail address: gcolldeforns@crm.cat

Luis Ortiz-Gracia
Universitat de Barcelona School of Economics
Faculty of Economics and Business
University of Barcelona
John M. Keynes 1-11
08034 Barcelona
Spain

E-mail address: luis.ortiz-gracia@ub.edu